

# Studying Impact of Unified Power Flow Controller on improve transient stability by Improved Harmony Search Algorithm

**Mehdi Nafar**

Department of Electrical Engineering, Marvdasht Branch, Islamic Azad University, Marvdasht, Iran

**Mostafa Abbasi**

Department of Electrical Engineering, Marvdasht Branch, Islamic Azad University, Marvdasht, Iran

**Mojtaba Abbasi**

Department of Electrical Engineering, Marvdasht Branch, Islamic Azad University, Marvdasht, Iran

## ABSTRACT

Main contribution of this work is improving transient stability by installing Flexible AC Transmission System (FACTS) in power systems. For do this, Unified Power Flow Controller (UPFC) has been selected. Also a novel structure has been suggested to improve classic Harmony Search algorithm and suggested improved Harmony Search (iHS) algorithm. This algorithm has been used to obtain UPFC parameters. Simulation has been performed by SIMULINK/MATLAB environment. Simulation results illustrate power and accuracy of the proposed technique.

## Keywords

Unified power flow controller, Harmony search algorithm, Transient stability improvement, Power system.

## 1. INTRODUCTION

In recent years, flexible AC transmission system devices are one of the most effective ways to improve power system operation controllability and power transfer limits. Through the modulation of bus voltage, phase shift between buses, and transmission line reactance, FACTS devices can cause a substantial increase in power transfer limits during steady-state [1].

The unified power flow controller is regarded as one of the most versatile devices in the FACTS device family [2-3] which has the ability to control of the power flow in the transmission line, improve the transient stability, mitigate system oscillation and provide voltage support. It performs this through the control of the in-phase voltage, quadrature voltage and shunts compensation due to its mains control strategy. The application of the UPFC to the modern power system can therefore lead to the more flexible, secure and economic operation [4].

In this paper, the published paper of UPFC have been classified in three categories, which are: placement and application as well as control.

Optimal sizing and siting of UPFC is complex problem

which has been solved by Group Search Optimization (GSO) algorithm, Gravitational Search Algorithm (GSA), Cat Swarm Optimization (CSO) algorithm, chemical reaction optimization algorithm and Particle Swarm Optimization (PSO) algorithm in [5-9], respectively.

Application of UPFC has been performed in three fields; which are oscillation damping [10-12], dynamic stability enhancement [13-14], load flow studies [15-17], relaying [18-20]. Control design is other challenge of researcher which is introduced in [21-23].

In this paper, the HBMO algorithm suggested for UPFC to damp oscillation and improve transient stability. This paper has been organized in five sections. Concept and modeling of UPFC has been introduced in section 2. The proposed technique for tuning UPFC are discussed in third section. Simulation results are available in section 4. This work has been concluded in section 5.

## 2. FORMULATION

### 2.1 UPFC concept

The basic components of the UPFC are two Voltage Source Inverters (VSIs) sharing a common dc storage capacitor, and connected to the power system through coupling transformers [24]. Shunt inverter or Static Compensator (STATCOM) is connected to system through a shunt transformer which injects varied controlled sinusoidal current in coupling point. STATCOM supplies line reactive power and simultaneously fix DC-voltage across DC-link. Series converter or SSSC regulates transmission power in desired value using controlled voltage phase and amplitude [25].

The shunt inverter is operated in such a way as to demand this dc terminal power (positive or negative) from the line keeping the voltage across the storage capacitor constant. So, the net real power absorbed from the line by the UPFC is equal only to the losses of the inverters and their transformers. The remaining capacity of the shunt inverter can be used to exchange reactive power with the line so to provide a voltage regulation at the connection

point [24-25]. The reactive power of the shunt converter can be controlled independently and modeled as a controllable shunt reactive power source. Therefore, to obtain the overall model, the injected reactive power to the bus  $i$  should be added to the series branch. In this model, UPFC is represented by two ideal voltage sources with series source impedances, connected in series and parallel with the transmission line, respectively, representing the output voltages of series and shunt branches of UPFC. However this model is highly suitable for the representation of UPFC in power flow studies, it does not take the operation losses into account in which the proposed method in this study accepts [26]. It consists of two back-to-back, self-commutated, voltage source converters connected through a common dc link [25]. Figure 1 shows the basic configuration of a UPFC.

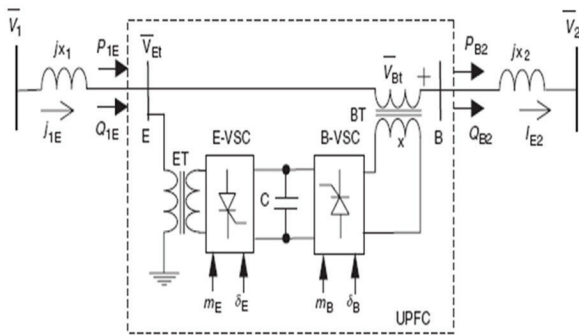


Figure 1. Configuration of a UPFC based on two back-to-back three-phase converters

### 2.2 UPFC modeling

Figure2 shows general model of connected UPFC to power system. In this paper, current injection model has been used for UPFC model. As illustrated in Figure3 is observed to model UPFC, voltage and current sources has been employed as series and shunt convertors, respectively.

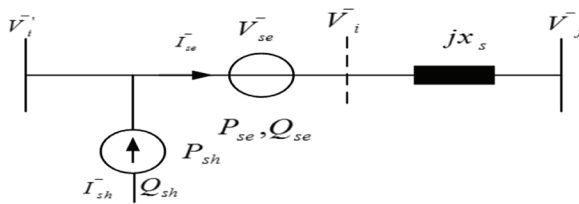


Figure 2. Equivalent circuit of UPFC converters in the transmission system

In Figure2, current of shunt convertor ( $I_{sh}$ ) can be decomposed to two components phase whit voltage  $V_i$  ( $I_i$ ) and perpendicular to it ( $I_q$ ) as following equation

$$\tilde{I}_{shunt} = \tilde{I}_t + \tilde{I}_q \tag{1}$$

$V_{se}$  is exchange-Series instead of an ideal voltage conversion,  $jx_{s1}$  and transmission reactance. Series voltage sources,  $V_{se}$ , are control variable phase and amplitude. Then, we have,

$$\tilde{V}_{s1} = M_B \tilde{V}_i e^{j\delta_E} \tag{2}$$

The injection current by UPFC obtains by converting voltage sources,  $V_{s1}$ , to current sources,  $I_{inj}$ . This facts has been illustrated in Figure3.

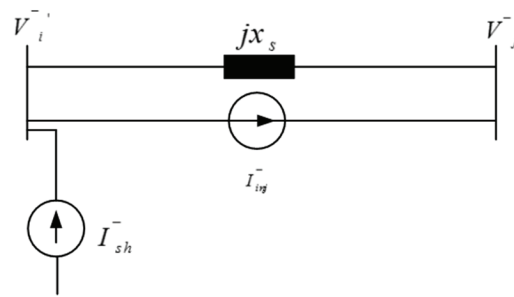


Figure 3. Current injection model of UPFC

By considering Figure3, we have:

$$\tilde{I}_{INJ} = \frac{\tilde{V}_s}{jx_s} = -jb_{s1} m_b \tilde{V}_i e^{j\delta_E} \tag{3}$$

where,  $b_{s1}=1/x_{s1}$  is susceptance of transmission line.  $M_B$  and  $\delta_E$  are phase and amplitude of injection voltage respect to voltage. Thus we can written,

$$P_{CONV1} = \text{Re} \left[ \tilde{V}_i \left( -\tilde{I}_{sh} \right) \right] = -V_i I_t \tag{4}$$

$$S_{s1} = \tilde{V}_{s1} \tilde{I}_{ij}^* = M_B \tilde{V}_i e^{j\delta_E} \left[ \frac{\tilde{V}_i - \tilde{V}_j}{j(x_{s1})} \right]^* \tag{5}$$

$$S_{s1} = P_{s1} + jQ_{s1} \tag{6}$$

Based on the above equations,

$$\begin{cases} P_{s1} = (b_{s1}) (M_B V_i V_j \sin(\theta_i - \theta_j + \delta_E) - M_B V_i^2 \sin(\delta_E)) \\ Q_{s1} = (b_{s1}) (M_B V_i V_j \cos(\delta_E) - 2M_B V_i^2 - M_B V_i V_j \cos(\theta_i - \theta_j + \delta_E)) \end{cases} \tag{7}$$

The absorbed active power by shunted convertor with power system is calculated by Eq.(8),

$$P_{shunt} = \text{Re} \left[ \bar{V}_i (-\bar{I}_{shunt}^*) \right] = -V_i I_i \quad (8)$$

From above equations, we have:

$$\begin{cases} -V_i I_i = (b_{s1}) (M_B V_j V_j \sin(\theta_i - \theta_j + \delta_E) - M_B V_i^2 \sin(\delta_E)) \\ \bar{I}_{shunt} = \bar{I}_i + \bar{I}_q = (b_{s1}) (-M_B V_j \sin(\theta_i - \theta_j + \delta_E) + M_B V_i \sin(\delta_E)) \end{cases} \quad (9)$$

So the UPFC injection model parameters according to the following Eq.3 are achieved.

$$\bar{I}_{Si} = \bar{I}_{shunt} - \bar{I}_{s1} \quad (10)$$

$$\bar{I}_{sj} = \bar{I}_{s2} \quad (11)$$

Finally, we can write

$$\bar{I}_{Si} = (b_{s1}) (-M_B V_j \sin(\theta_i - \theta_j + \delta_E) + M_B V_i \sin(\delta_E)) + b_{s2} M_B \bar{V}_i e^{\delta_E} \quad (12)$$

$$\bar{I}_{Sj2} = -j b_{s2} M_B \bar{V}_i e^{\delta_E} \quad (13)$$

### 3. IMPROVED HARMONEY SEARCH ALGORITHM

Harmony Search (HS) algorithm has been proposed by Geem et al. in 2001 [27]. HS algorithm has been suggested based on musical improvisation process.

#### 3.1 HS algorithm Definitions

Before starting the HSA, a number of parameters should be defined,

- The number of Iterations (IN) which is determined by complexity and nature of problem.
- The number of Decision Variables (DVN), which set of these DVNs constitute a harmony.
- Size of harmony search (SHS) used to specify the number of harmonies that will be stored in the harmony memory.
- Pitch Adjustment Rate (PAR) determines probability value to get decision values. By adding a determined value, these values are copied from a harmony in memory.
- Harmony Memory Considering Rate (HMCR) determines the rate at which decision variables in the harmony are considered as elements of a new harmony that will be created. This parameter is determined between [0, 1].

#### 3.2 Simple HS Structure

In classic structure, HS algorithm has five steps,

*Step i.* Initializing problem and parameters: Main goal to use this algorithm is minimizing the objective function,  $f(U)$ , that is a vector with the size of decision variables,  $N$ , then

$$\begin{aligned} & \text{Min} \{f(\bar{U})\} \\ & u_i \in U_i, i = 1, 2, \dots, N \end{aligned} \quad (14)$$

where,  $U_i$  is a possible vector of values for each decision variable with the size of PAR.

*Step ii.* Initializing harmony memory: HS is a population based algorithm. This algorithm is started using an initial matrix. Dimensions of this matrix are determined by the number of decision variables and harmony memory size. Thus, Harmony Memory (HM) is obtained by following matrix,

$$\bar{M} = \begin{bmatrix} U_1^1 & U_2^1 & \dots & U_{N-1}^1 & U_N^1 \\ U_1^2 & U_2^2 & \dots & U_{N-1}^2 & U_N^2 \\ \vdots & \vdots & \ddots & \vdots & \vdots \\ U_1^{SHS-1} & U_2^{SHS-1} & \dots & U_{N-1}^{SHS-1} & U_N^{SHS-1} \\ U_1^{SHS} & U_2^{SHS} & \dots & U_N^{SHS} & U_N^{SHS} \end{bmatrix} \quad (15)$$

*Step iii.* Improvising a new harmony: A new harmony is generated according to memory consideration with a probability of  $HMCR$ . Then, new harmony is produced as  $U' = [u1', u2', u3', \dots, uN']$ . PAR adjusts parameter from memory consideration. Three important rules are considered to generate new harmony vector, i.e. (a) memory consideration, (b) pitch adjustment, and (c) random selection.

To generate new vector, the value of first decision variable ( $U1NEW$ ) and other decision variables ( $U2NEW, U3NEW, \dots, UNNEW$ ) are selected from values in the specified HM range based on  $HMCR$ ,

$$U_i^{NEW} = \begin{cases} U_i^{NEW} \in \{U_i^1, U_i^2, \dots, U_i^{HMS}\} & \text{if } HMCR \\ U_i^{NEW} \in U_i & \text{if } 1 - HMCR \end{cases} \quad (16)$$

any obtained components by the memory consideration is examined to determine whether it should be pitch-adjusted or not. This operation uses the  $PAR$  parameter, which is the rate of pitch adjustment as Eq. (14):

$$\text{Pitch adjusting decision for } U_i^{NEW} \leftarrow \begin{cases} \text{Yes} & f < PAR \\ \text{No} & f \geq 1 - PAR \end{cases} \quad (14)$$

The value of (1 - PAR) sets the rate of doing nothing. If the pitch adjustment decision for  $U_i^{NEW}$  is YES,  $U_i^{NEW}$  is replaced as Eq. (15):

$$U_i^{NEW} \leftarrow U_i^{NEW} \pm \text{rand}(0,1) \times BW \quad (15)$$

where, BW is an arbitrary distance bandwidth.

Step iv. Updating HM: In this step, updating process is done based on solution of objective function. In other words, if related solution of new obtained harmony vector is better than the worst harmony vector in the HM, this vector is selected.

Step v. Termination criteria: To terminate algorithm, there is two techniques: reach to optimal solution and finishing iteration number. In the most optimization problem, second criterion is used.

### 3.3 Self-adaptive Global best HS Algorithm

To obtain better solution in comparison to simple HS algorithm, several improvement techniques have been suggested. These techniques mainly are categorized in two groups. The goal of first group is adapting control parameters of HS algorithm. Second category has focused on change structure of simple HS algorithm operators and/or adding new operator. In this paper, a method of first category has been used to improve simple HS algorithm. In the SGHS algorithm, four control parameters HMS, HMCR, PAR and BW are closely related to the problem being solved and the phase of the search process which may be either exploration or exploitation. In this paper, HCMR and PAR are dynamically adapted to a suitable range by recording their historic values corresponding to generated harmonies entering the HM. We assume that the HMCR (PAR) value is normally distributed in the range of [0.9, 1.0] ([0.0, 1.0]) with mean HMCRm (PARm) and standard deviation 0.01 (0.05). Initially, HMCRm (PARm) is set at 0.98 (0.9). And then SGHS starts with a HMCR (PAR) value generated according to the normal distribution. During the evolution, the HMCR (PAR) value associated with the generated harmony successfully replacing the worst member in the HM is recorded.

After a specified number of generations LP (i.e., the learning period which is 100 in our experiment), HMCRm (PARm) is recalculated by averaging all the recorded HMCR (PAR) values during this period. With the new mean and the given standard deviation of 0.01 (0.05), new HMCR (PAR) value is produced and used in the subsequent iterations. The above procedure is repeated. As a

result, an appropriate HMCR (PAR) value can be gradually learned to suit the particular problem and the particular phases of the search process.

The parameter BW is a distance bandwidth for the continuous design variable. A large BW value is in favor of the algorithm searching in a large scope, while a small BW value is appropriate for fine-tuning of the best solution vectors. To well balance the exploration and exploitation of the proposed SGHS algorithm, the BW value decreases dynamically with increasing generations (IN) as follows:

$$BW = \begin{cases} BW_{\max} - \frac{BW_{\max} - BW_{\min}}{IN} \times 2gen & \text{if } gen < IN / 2 \\ BW_{\min} & \text{if } gen \geq IN / 2 \end{cases} \quad (16)$$

where,  $BW_{\max}$  and  $BW_{\min}$  are the maximum and minimum distance bandwidths, respectively. gen is the number of generation.

The SGHS algorithm does not require a precise setting of specific values to critical parameters HMCR, PAR and BW in accordance with problem's characteristic and complexity. These parameters are self-adapted by a learning mechanism or dynamically decreased with generation counter. Therefore, the SGHS algorithm can demonstrate consistently good performance on problems with different properties [28].

## 4. CASE STUDY

In this section, simulation results are presented in several figures. Simulation has been performed by Matlab 2010 software. First, optimal values for simulation are extracted by HBMO algorithm using coding in mfile environment. Then, process extraction results are completed by applying the values to Simulink environment.

### 4.1 Simulation implementation

In simulation process, the HBMO algorithm has been used for tuning and extracting optimal values of constant parameters. The desired curves obtain by linking results coding of mfile to Simulink. Figure4 shows location of UPFC in power system. It is assumed that UPFC has been installed between buses B1 and B2. Buses B1 and B2 have been connected to source and network, respectively.

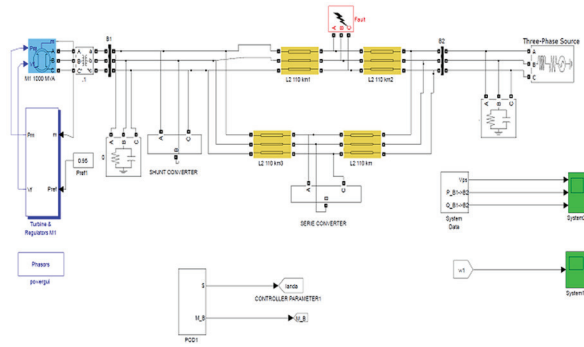


Figure 4. General Structure of sample system

### 4.1.1 General Characteristics of Synchronous Generator

Energy source of system is a three phase machine 1000 MVA, line to line voltage 13.8 kV and frequency 60 Hz. Values of reactance  $X_d$ ,  $X'd$ ,  $X_q$  and  $X'q$  in pu are 0.296, 0.252, 0.474 and 0.243, respectively. Stator resistance is  $2.8544 \times 10^{-3}$  pu. Value of internal factor ( $H(s)$ ) and the number of pole pair of machine are 3.7 and 32, respectively.

### 4.1.2 General specifications of the turbine

The used generator rotates by a turbine. Figure5 shows structure of turbine and regulator. This block diagram consists of a mechanical input, hydraulic turbine and governor and excitation system.

#### a. Hydraulic turbine and governor

- Servo-motor  
The gain  $K_a$  and time constant  $T_a$ , in seconds (s), of the first-order system representing the servomotor. In this case,  $K_a$  and  $T_a$  are 10.3 and 0.07 second, respectively.
- Gate opening limits  
The limits  $g_{min}$  and  $g_{max}$  (pu) imposed on the gate opening, and  $vg_{min}$  and  $vg_{max}$  (pu/s) imposed on gate speed, which are 0.01, 0.97518, -0.1 and 0.1, respectively.
- Permanent droop and regulator  
The static gain of the governor is equal to the inverse of the permanent droop  $R_p$  in the feedback loop. The PID regulator has a proportional gain  $K_p$ , an integral gain  $K_i$ , and a derivative gain  $K_d$ . The high-frequency gain of the PID is limited by a first-order low-pass filter with time constant  $T_d$  (s). Values of  $R_p$ ,  $K_p$ ,  $K_i$ ,  $K_d$  and  $T_d$  are 0.05, 1.163, 0.105, 0 and 0.01, respectively.
- Hydraulic turbine  
The speed deviation damping coefficient  $\beta$  and water starting time  $T_w$  (s), which are equal to 0 and 2.67, respectively.
- Initial mechanical power  
The initial mechanical power  $Pm0$  (pu) is equal to 0.952577. This value is automatically updated by the load

flow utility of the Powergui block.

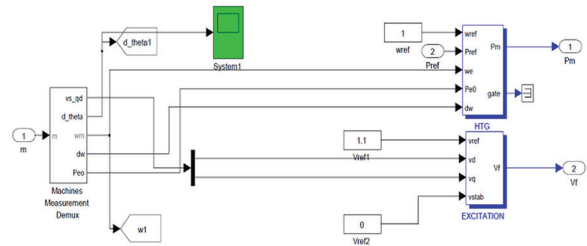


Figure 5. Structure of the connected turbine to Synchronous Generator

#### b. Excitation system

The exciter is represented by the following transfer function between the exciter voltage  $V_{fd}$  and the regulator's output  $E_f$ :

$$\frac{V_{fd}}{E_f} = \frac{1}{K_e + sT_e} \quad (19)$$

- Low-pass filter time constant  
The time constant  $T_r$ , in seconds (s), of the first-order system that represents the stator terminal voltage transducer which is  $20 \times 10^{-3}$  second.
- Regulator gain and time constant  
The gain  $K_a$  and time constant  $T_a$ , in seconds (s), of the first-order system representing the main regulator. The values of  $K_a$  and  $T_a$  are 200 and 0.001 second, respectively.
- Exciter  
The gain  $K_e$  and time constant  $T_e$ , in seconds (s), of the first-order system representing the exciter are 1 and 0, respectively.
- Transient gain reduction  
The time constants  $T_b$ , in seconds (s), and  $T_c$ , in seconds (s), of the first-order system representing a lead-lag compensator and both are considered zero.
- Damping filter gain and time constant  
The gain  $K_f$  and time constant  $T_f$ , in seconds (s), of the first-order system representing a derivative feedback. The values of these parameters are 0.001 and 0.1, respectively.
- Regulator output limits and gain  
Limits  $E_{fmin}$  and  $E_{fmax}$  are imposed on the output of the voltage regulator. The upper limit can be constant and equal to  $E_{fmax}$ , or variable and equal to the rectified stator terminal voltage  $V_{t1}$  times a proportional gain  $K_p$ . If  $K_p$  is set to 0, the former applies. If  $K_p$  is set to a positive value, the latter applies. The applied values to  $E_{fmin}$ ,  $E_{fmax}$  and  $K_p$  are zero, 7 and zero, respectively.
- Initial values of terminal voltage and field voltage  
The initial values of terminal voltage  $V_{t0}$  (pu) and field voltage  $V_{f0}$  (pu). When set correctly, they allow you to

start the simulation in steady state. Initial terminal voltage should normally be set to 1 pu. Both  $V_{i0}$  and  $V_{j0}$  values are automatically updated by the load flow utility of the Powergui block.

4.1.3 Transmission system

The transmission system is a grounded star system which line to phase voltage (in  $kV$ ), nominal frequency (in  $Hz$ ), active power (in  $kW$ ) and capacitive reactive power (in  $KVAr$ ) are 20, 60, 125 and 1000, respectively.

4.1.4 Three phase source

Effective phase to phase voltage (in  $kV$ ), frequency (in  $Hz$ ), source resistance (in  $\Omega$ ) and source reactance (in  $H$ ) are 500, 60, 0.8929 and  $16.58 \times 10^{-3}$ .

4.2 Simulation results

Fig 6 illustrates dynamic response for speed. By considering the figure, it can be claimed damping obtains in all cycles except first cycle. The maximum and minimum bounds are 1.025 and -0.96, respectively.

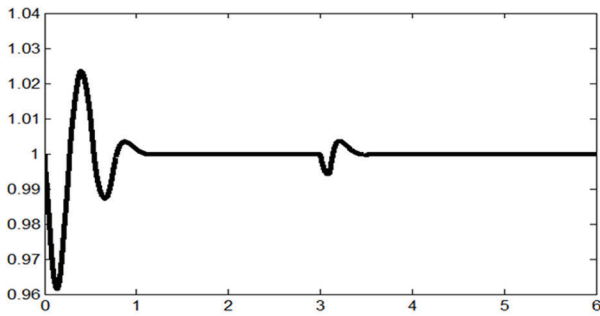


Figure 6. Dynamic response for speed

Figure 7 shows transformed power between buses B1 and B2 where UPFC has been installed. By focusing in this figure it can be claimed that however a distortion happens in middle cycles but in the rest places, curve is returned to 5000. In the beginning, this amount reached more than 16000.

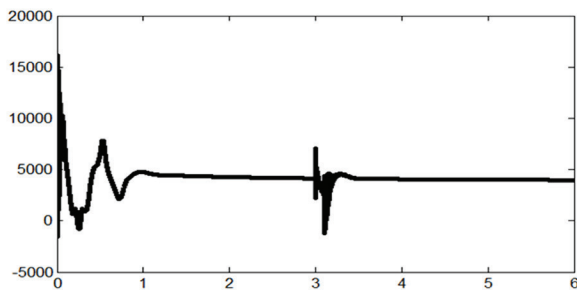


Figure 7. Transformed power between two buses

Changes in the control parameter lambda are visible in Figure 8. You could say the behavior is similar to the curve 7. Maximum and minimum range is respectively 9 and 6.

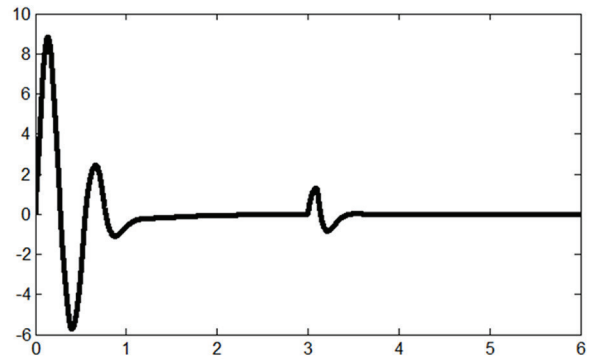


Figure 8. Changes in the control parameter lambda

Finally, voltages of buses B1 and B2 are visible in Figure 9.

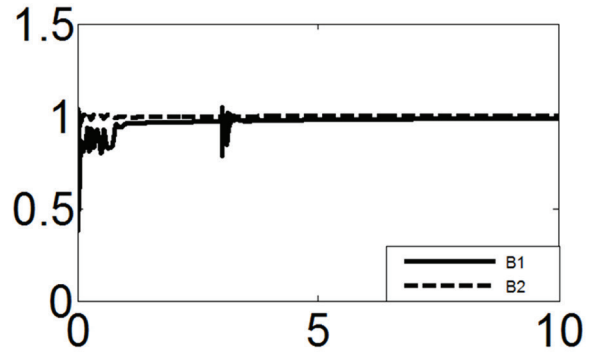


Figure 9. Voltages of Buses B1 and B2

CONCLUSION

In this paper, dynamic behavior problem of power system has been improved by installing UPFC. One of the main challenge has been considered in problem formulation; i.e. oscillation damping and transient stability improvement. The problem has been optimized by HBMO algorithm. Four parameters have been considered in extraction results, which are: dynamic response for speed, transformed power between two buses, changes in the control parameter lambda and voltages of buses B1 and B2. From simulation results which visible in Figs. 6-9, it can be claimed that distortion usually occurs in mid-cycle. The first cycle is the worst possible response and extreme distortions. The two curves of dynamic response for speed and transformed power between two buses have a similar behavior.

## REFERENCE

- 1) Al-Awami A.T., Abdel-Magid Y.L., & Abido MA. (2007). A particle-swarm-based approach of power system stability enhancement with unified power flow controller. *Electric Power Energy System*, vol.29, pp.251–259.
- 2) Gyugyi, L. (1992). Unified power-flow control concept for flexible ac transmission systems. *IEE Proc Gen Transm Distrib*, vol. 139, no.4), pp.323–231.
- 3) Hingorani, N.G., & Gyugyi, L. (1999) Understanding FACTS: concepts and technology of flexible AC transmission systems. Wiley-IEEE Press, USA.
- 4) Shayeghi, H., Shayanfar, H.A., Jalilzadeh S., & Safari, A. (2010). Tuning of damping controller for UPFC using quantum particle swarm optimizer. *Energy Conversion and Management*. vol.51, pp.2299-2306.
- 5) Tarafdar-Hagh, M., Alipour, M., & Teimourzadeh, S. (2014). Application of HGSO to security based optimal placement and parameter setting of UPFC, *Energy Conversion and Management*, Vol. 86, pp. 873-885
- 6) Sarker, J., & Goswami, S.K. (2014). Solution of multiple UPFC placement problems using Gravitational Search Algorithm, *International Journal of Electrical Power & Energy Systems*, Vol. 55, pp. 531-541
- 7) Naveen Kumar, G., Surya Kalavathi, M. (2014). Cat Swarm Optimization for optimal placement of multiple UPFC's in voltage stability enhancement under contingency, *International Journal of Electrical Power & Energy Systems*, Vol. 57, pp. 97-104.
- 8) Dutta, S., Kumar Roy, P., Nandi, D. (2015). Optimal location of UPFC controller in transmission network using hybrid chemical reaction optimization algorithm, *International Journal of Electrical Power & Energy Systems*, Vol. 64, pp. 194-211
- 9) Hajforoosh, S., Nabavi, S.M.H., & Masoum, M.A.S. (2012). Coordinated aggregated-based particle swarm optimisation algorithm for congestion management in restructured power market by placement and sizing of unified power flow controller, *IET Science, Measurement & Technology*, Vol.6 , No. 4, pp. 267-278.
- 10) Shotorbani, A.M., Ajami, A., Aghababa, M.P., & Hosseini, S.H. (2013). Direct lyapunov theory-based method for power oscillation damping by robust finite-time control of unified power flow controller, *IET Generation, Transmission & Distribution*, Vol. 7, No, 7, pp. 691 – 699.
- 11) Kasinathan, P., Vairamani, R., Sundramoorthy, S. (2013). Dynamic performance investigation of d-q model with PID controller-based unified power-flow controller, *IET Power Electronics*, Vol. 6, No. 5, pp. 843-850.
- 12) Golshannavaz, S., Aminifar, F., & Nazarpour, D. (2014). Application of UPFC to Enhancing Oscillatory Response of Series-Compensated Wind Farm Integrations , Smart Grid, *IEEE Transactions on* , Vol. 5, No. 4, , pp. 1961-1968.
- 13) Wang L., Li H.-W., Wu Ch.-T. (2013). Stability Analysis of an Integrated Offshore Wind and Seashore Wave Farm Fed to a Power Grid Using a Unified Power Flow Controller, *IEEE Transactions on Power Systems*, Vol. 28, No. 3, pp. 2211-2221.
- 14) Vijay Kumar, B., & Srikanth, N.V. (2015) Optimal location and sizing of Unified Power Flow Controller (UPFC) to improve dynamic stability: A hybrid technique, *International Journal of Electrical Power & Energy Systems*, Vol. 64, pp. 429-438
- 15) Kamel, S., Jurado, F., & Peças Lopes, J.A. (2015) Comparison of various UPFC models for power flow control, *Electric Power Systems Research*, Available online 25 November. Vol. 121, pp.243-251.
- 16) Ajami, A., Shotorbani, A.M., & Aagababa, M.P. (2012). Application of the direct Lyapunov method for robust finite-time power flow control with a unified power flow controller, *IET Generation, Transmission & Distribution*, Vol.1, pp.822-830.
- 17) Mohammadpour Sh., Ajami, A., Zadeh, A., Aghababa, S.G., & Mahboubi, M.P. (2014) Robust terminal sliding mode power flow controller using unified power flow controller with adaptive observer and local measurement, *IET Generation, Transmission & Distribution*, Vol. 8, No. 10, pp.1712-1723.
- 18) Rahul Dubey, S.R., Samantaray, B.K., Panigrahi, G.V. (2015). Adaptive distance relay setting for parallel transmission network connecting wind farms and UPFC, *International Journal of Electrical Power & Energy Systems*, Vol. 65, pp. 113-123.
- 19) Tripathy, L.N., Kumar Jena, M., & Samantaray, S.R. (2014) Differential relaying scheme for tapped transmission line connecting UPFC and wind farm, *International Journal of Electrical Power & Energy Systems*, Vol. 60, pp. 245-257

- 20) Dubey, R., Samantaray, S.R., & Panigrahi, B.K. (2014). Simultaneous impact of unified power flow controller and off-shore wind penetration on distance relay characteristics, *IET Generation, Transmission & Distribution*, Vol. 8, No. 11, pp.1869-1880.
- 21) Vervecken, J., Silva, F., Barros, D., Driesen, J. (2012). Direct Power Control of Series Converter of Unified Power-Flow Controller With Three-Level Neutral Point Clamped Converter, *IEEE Transactions on Power Delivery*, Vol. 27, No. 4, pp. 1772-1782.
- 22) Farrag, M.E.A., & Putrus, G.A. (2012) Design of an Adaptive Neurofuzzy Inference Control System for the Unified Power-Flow Controller, *IEEE Transactions on Power Delivery*, Vol. 27, No. 1, pp.53-61.
- 23) Monteiro, J., J.F., Silva, S.F., Pinto, J., & L., Palma. (2014) Linear & Sliding-Mode Control Design for Matrix Converter-Based Unified Power Flow Controllers, *IEEE Transactions on Power Electronics*, Vol. 29, No. 7, pp. 3357-3367.
- 24) Tara Kalyani, S., & Tulasiram Das, G. (2008). Simulation of Real and Reactive Power Flow Control with UPFC Connected to a Transmission Line, *Journal of Theoretical and Applied Information Technology*, Vol.3, pp.11-20.
- 25) Mailah, N.F., Bashi, N.Marium, S.M., & Aris, I. (2008). Simulation of a three-Phase Multilevel Unified Power Flow Controller UPFC, *Journal of Applied Scientific*, Vol. 8, pp.96-104.
- 26) Mete Vural, A., Tumay, M. (2007), Mathematical Modeling and Analysis of a Unified Power Flow Controller: A Comparison of Two Approaches in Power Flow Studies and Effects of UPFC Location, *Electrical Power and Energy Systems*, Vol. 29, pp.114-121.
- 27) Geem, Z.W., Jim, J.H., & Loganathan G.V. (2001). A new heuristic optimization algorithm: harmony search, *Simulation*, Vol.72, No.2, pp. 60-68.
- 28) Morsali, R., Jafari, T. Ghods, A., Karimi, M. (2014). Solving unit commitment problem using a novel version of harmony search algorithm, *Frontiers in Energy*, Vol.8, No.3, pp. 297-304.